JOURNAL OF PROPULSION AND POWER
Vol. 17, No. 5, September–October 2001

Russian Research on Experimental Hydrogen-Fueled Dual-Mode Scramjet: Conception and Preflight Tests

Donat A. Ogorodnikov,* Viacheslav A. Vinogradov,† Yurii M. Shikhman,‡ and Vitaliy N. Strokin†
Central Institute of Aviation Motors, 111250, Moscow, Russia

The experience of model dual-mode scramjet (DMSCRAM) creation and the main results of ground and preflight tests are analyzed in this paper beginning from the conception choice, goals, and working program implemented for about 15 years, preceding to the first flight test of hypersonic flight laboratory. Design schemes for plane and axisymmetrical engine concept are examined. The description of experimental test facilities, test instrumentation, and methods of readings treatment used in ground-test procedure of DMSCRAM are given. The test results of ground model engine at Mach-number range $M = 3.5$–6.5 and ground test-results for flight type engine at $M = 5$ were cited and confirmed the durability and readiness of developed DMSCRAM for flight tests.

Nomenclature

C_R	=	thrust coefficient, $C_R = R/(q_\infty \times F_{\text{inlet}})$
C_X	=	drag coefficient, $C_X = X/(q_\infty \times F_{\text{inlet}})$
F	=	cross-section area
G	=	mass fuel, air rate
g	=	relative fuel consumption
I	=	flow impulse
M	=	Mach number
P_Q	=	heat release parameter
Q_{comb}	=	heat resulted in fuel combustion
Q_W	=	summary heat flux into the duct walls
q_w	=	specific heat flux into the wall
q_∞	=	freestream dynamic pressure
R	=	thrust
Re	=	Reynolds number
T	=	temperature
X	=	drag force
α	=	angle, heat-transfer coefficient
β	=	fuel/air equivalence ratio
δ_α	=	heat-transfer nonuniformity coefficient, $\delta_{\alpha,\text{cool}} = (\alpha_{\max} - \alpha_{\min})/\alpha_{\text{average}}$
η	=	combustion efficiency
ξ_Σ	=	nozzle impulse loss coefficient, $\xi_\Sigma = (1 - I_{\text{real}}/I_{\text{ideal}})$
σ	=	total pressure recovery coefficient
φ	=	inlet capture ratio

Subscripts

at	=	angle of attack
c, comb	=	combustor
cool	=	cooling system, coolant
rz	=	recirculation zone
t	=	total parameters
th	=	inlet throat
w	=	wall
Σ	=	summary value
I, II, III, IV, and V	=	rows of fuel injectors
∞	=	freestream parameters

Presented as Paper 98-1586 at the AIAA 8th International Space Planes and Technologies Conference, Norfolk, VA, 27–30 April 1998; received 29 October 1998; revision received 3 March 2001; accepted for publication 12 March 2001.

*CIAM Honorary Director, Academician, 2 Aviamotornaya Street.
†Head of Department, 2 Aviamotornaya Street. Member AIAA.
‡Head of Section, 2 Aviamotornaya Street.

I. Introduction

THE interest in the development of high-speed ramjet engines, especially supersonic combustion ramjet (SCRAM) engines, and its utilization for space transportation leads inevitably to a question about flight tests to check its durability and to validate theoretical and ground-test results. Flight tests were necessary because of the impossibility of reproducing real flight conditions at ground tests, even with tests in shock and impulse tubes. SCRAM flight tests were first planned in USA in the 1960s.[1] It was planned to use the X-15 plane as a booster and then as a vehicle, but the work did not continue through the flight tests because of funding shortcuts.

In the USSR the preparation of flight tests was focused on designing and manufacturing of hydrogen-fueled SCRAM and its elements beginning from the 1970s.[2] It was planned to install the SCRAM engine and its equipment (fuel and control systems, instrumentation, and so on) on a hypersonic flight laboratory (HFL) vehicle. There were two possible ways for the HFL launching: by aircraft or rocket, but finally rocket launching was chosen to accelerate the HFL up to the hypersonic velocities. E. S. Shchetinkov was the initiator of flight tests in the USSR with the supervision D. A. Ogorodnikov, V. A. Sosounov, and R. I. Kurziner of CIAM.

The main purposes of the flight tests are 1) to check the possibility for effective working process in SCRAM and stable joint operation of its elements; 2) to test engine cooling system at operation on real fuel, liquid hydrogen (LH_2); 3) to design and to test fuel tank, control, and feed systems; 4) to check the principle of engine control and engine LH_2 fuel system operation and to meet the possibility of engine restart; 5) to check the reliability of engine construction and utilized materials; and 6) to check the operation of onboard data acquisition and processing systems. All of these issues added several requirements (conflicting sometimes) on the engine system development and on the choice of airflow channel. Figure 1 shows the photo of the rocket with SCRAM in composition of HFL.

II. Engine Concept for Flight Tests

The trajectory of HFL and Reynolds number (Re) variation vs flight time are depicted in Fig. 2, along with the parameters at the beginning and end of the engine operation during the flight. The engine operating range is bounded with Mach number from $M = 3.5$–4 to $M = 5.3$–5.9 at altitudes $H = 11$–27 km during $\approx$120 s for the nominal trajectory of rocket with HFL. Moreover, the Reynolds number based on a dimension of 0.2 m varies from 5×10^5 up to 10^6. Taking into account the dispositions of engine at the nose of the rocket and the possible rocket rotation, the angle of attack for airflow entering the inlet was chosen to be equal to 5 deg.

It is well known that, at low hypersonic speeds of $M = 3$–8, the dual-mode scram (DMSCRAM), operating as ramjet or as scram depending on flight velocity and engine operation mode, is one of

Fig. 1 Experimental DMSCRAM installed on rocket: 1, DMSCRAM; 2, "surface-air" rocket.

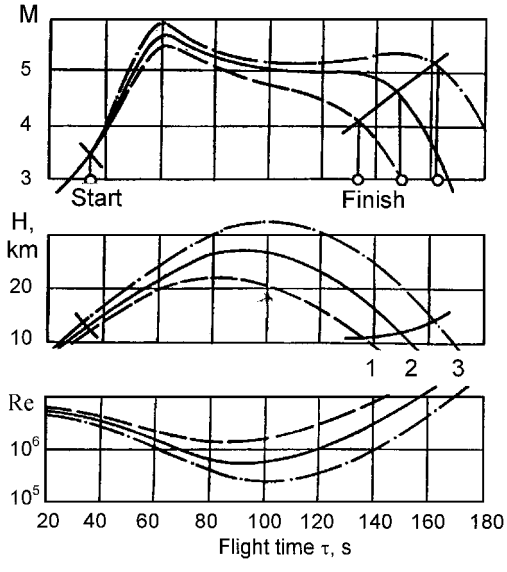

Fig. 2 Flight trajectories of HFL: 1, nominal trajectory; 2, low trajectory; 3, high trajectory.

the optimal type of engine. However, at $M > 4$ the high heat loading made airflow channel control almost impossible, and consequently fixed-geometry engines were used. The scheme exists for a flight-test engine with a combined combustor in which a subsonic condition fuel is injected and burns in the expanded part; near the end of combustor with a cross section more than inlet throat (subsonic combustion) and at supersonic conditions (supersonic combustion), fuel is injected near the entrance of combustor and burns along the whole its length was chosen for the analysis of such an engine schemes.[3]

In accordance with the DMSCRAM approaches existing in those times, the rectangular mode of engine was chosen for the first step of investigation. In later steps, however, an axisymmetrical model with annular combustor was chosen, mainly to simplify the HFL

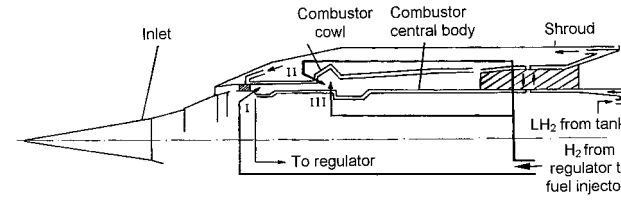

Fig. 3 Flight DMSCRAM conception.

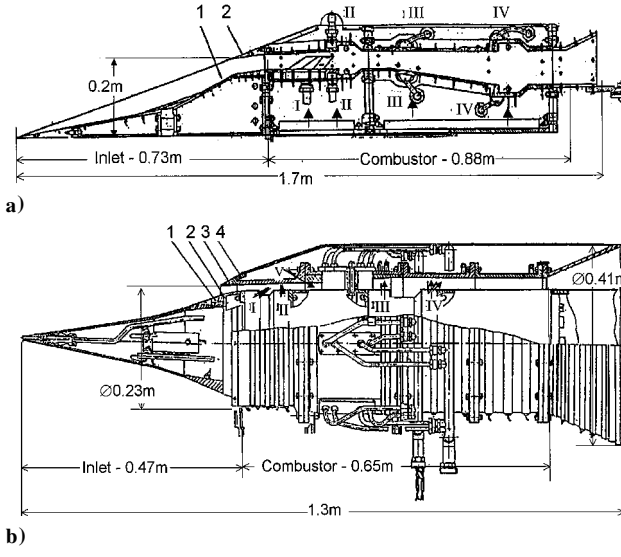

Fig. 4 Schemes of experimental models: a) two-dimensional engine and b) axisymmetrical engine; arrows point fuel row injector position, units 1–4 (inlet spike and cowl lip) are removed in case of direct-connect tests.

construction, to decrease the weight of HFL with engine, and to decrease the cost of engine development and finishing treatment.

Following with the flight-test requirements and goals, the engine construction was preceded by the development and creation of its elements (inlet, combustor, nozzle) and its systems: ignition, cooling, fuel feeding, control, diagnostic and instrumentation, and so on (Fig. 3). It was planned in preflight tests to test in ground facilities these elements and systems and also engine models and the final version of DMSCRAM flight engine.

III. Engines Design for Ground and Flight Tests

The design and manufacturing of rectangular DMSCRAM models were conducted at CIAM and the same for axisymmetrical models—in Design Bureau "Soyus" under the technical requirements of CIAM.[3] The walls of ground models were made of stainless steel without cooling. To determine the possibility of ground tests for the rectangular model, a full-scale DMSCRAM mock-up was fabricated. Figure 4 shows schematically the rectangular and axisymmetrical engines.

The rectangular DMSCRAM model measures a length $L = 1.7$ m and an inlet cross-section area of 0.2×0.2 m^2 and consists of an inlet, a combustor, and a short nozzle (see Fig. 4a). The dimension for the three-shock, fixed-geometry inlet with a total wedge angle 25 deg and a reference throat area of $\bar{F}_{\text{th}} = 0.2$ was chosen for $M = 6$. The combustor has a constant height of 0.2 m and comprises three sections: the first of $L = 0.38$ m with a cross-section area of $F_1 = 0.009$ m^2, the second with an exit cross-section area of $F_3 = 0.016$ m^2, and the third with $F_3 = \text{const}$ and $L_3 = 0.2$–0.35 m. Hydrogen was injected from upper and bottom walls and from struts through four injector rows, located at the entrance of each combustor section. Hydrogen ignition was accomplished by electrical spark plugs mounted in wall cavity stabilizers in the first and in the third combustor sections.[3]

The axisymmetrical DMSCRAM model (see Fig. 4b) had a length ≈ 1.3 m and was designed by taking into consideration the test results

for the rectangular one. The cross-section area and the design Mach number for the three-step inlet was the same at $\bar{F}_{\text{th}} = 0.195$. The shape of the combustor was almost the same as that for rectangular DMSCRAM, but the length of the third part of combustor and the number of fuel nozzles were enlarged as a result of rectangular DMSCRAM tests. Fuel injection was performed through five rows of injectors on the bottom (I–IV rows) and upper walls (V row). Fuel ignition was obtained by electrical sparkplugs located in cavity flame stabilizers at the entrance of the second (on the cowl) and the third (on the central body) parts of combustor. The forward and rearward edges of the force struts connecting the central body and cowl were cooled by water. The engine nozzle imitates the expansion ratio of the nozzle of engine flight type duct with $\bar{F}_{\text{noz}} = 2$.

The engine for flight tests on the HFL was also performed in the Design Bureau "Soyus" under technical requirements of CIAM, taking into consideration the results of ground tests for engines and its elements and systems. To allow stable operation of the engine at low Mach flight numbers, the cross-section area for the third section of the combustor was enlarged more than 1.5 times in comparison with the ground-test engine. The sparkplugs were installed within cavity flame stabilizers of the second and the third hydrogen injection rows. The construction scheme of engine had been also changed.

Figure 5 shows the photos of the ground- and flight-test models. The engine was fastened to the rocket through transition junctions that require special tests on the influence of flow squeezing.

IV. Investigation of DMSCRAM Elements and Systems

The investigation of elements and systems for hydrogen-fueled DMSCRAM forestalled the development of model engines and engines for flight tests. Additional data about the combined operation of elements were obtained at ground tests also. The data was used in the design and manufacturing of flight engines.

A. Inlet and Engine Duct Gasdynamics

Selection of the inlet configuration and its main dimensions were carried out based on a parametric theoretical study.[4] The code used for study of flowfield in engine duct was based on Euler equations for inviscid flow and integral boundary-layer equation and iterative procedure of viscous-inviscid interaction. To determine the characteristics of the flowfield within the airflow passage with and without the transition junction, several inlet models were tested at scales of $M1{:}2$ and $M1{:}4$, (see Fig. 6). The models were instrumented with static pressure taps, total pressure rakes, thermocouples, metered nozzles, and throttle devices. The schlieren method was used to visualize the flow around the inlet. Experimental investigations were carried at the CIAM and TsAGI test facilities at the $\alpha_{\text{at}} = 0$–5 deg in the range of $M = 1.75$–6 for the axisymmetrical and of $M = 2$–8 for the rectangular engine versions.

The inlet throat area, cowl and central body radii, and airflow passage configuration were varied in the tests. To simulate the heat-addition phenomena in the combustor, the airflow choking was achieved by either gas injection or a throttling device up to the stall condition at the engine entrance. Initial and repeatable starting conditions for the inlet were determined at experimental investigation. Besides, inlet performance and total pressure losses in airflow passage were determined at ground tests. It was determined that at $M = 3.5$–6 and $\alpha_{\text{at}} = 0$–5 deg, the inlets for the rectangular and axisymmetrical engines had been started, and the flowfield in the entrance corresponded to the design one. An example of inlet characteristics for the axisymmetrical DMSCRAM is given in Figs.7 and 8.

B. Investigation of Ignition and Combustion Process in Model Combustors

The studies of ignition, flame stabilization, and, finally, on gaseous hydrogen burning within model combustors were performed in CIAM under connected-pipe conditions at $M_{\text{air}} = 2$–3, $P_{t,\text{air}} = (5\text{–}20) \times 10^5$ Pa, $T_{t,\text{air}} = 900$–3000 K and in DMSCRAM model.[5–7] Model combustors of various fashion with wall and strut

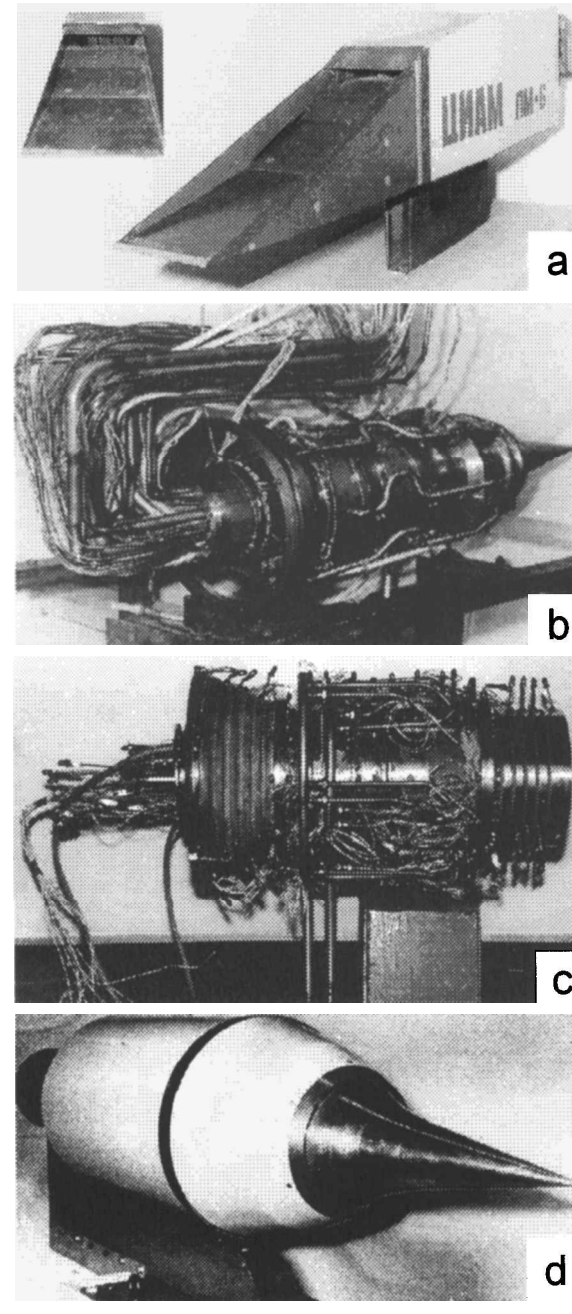

Fig. 5 Photos of test engines: a) Two-dimensional DMSCRAM (side and frontal views), b) Axisymmetrical DMSCRAM for freejet tests, c) Axisymmetrical DMSCRAM for direct-connect tests, and d) Stend variant of flight DMSCRAM.

fuel injection under chemical or plasma air heating were used. Results revealed that ignition of hydrogen in supersonic flows with rather low temperature and pressure ($M_{\text{air}} = 2$–3, $T_{t,\text{air}} < 900$ K, $P_{\text{air}} = 15$–30 kPa) could be met with the help of an electrical spark plug mounted in the wall cavity by means of a capacitance ignition system with high energy, ≈2.5 J. The criterion of ignition was found that allowed development of the ignition system for model and flight engines. The tests revealed that hydrogen self-ignition depends not only on airflow parameters, but on airflow structure in combustor; the presence of shocks and separation zones render the ignition easier to a great extent.

To provide stable combustion process of hydrogen jets in supersonic flow, the cavity flameholders were developed and investigated. By analyzing the large amount of cavity stabilization data, a stabilization criterion K_s ($K_s = U_{\text{air}}/(P_{\text{rz}}^{1.45} \times T_{t,\text{air}}^{2} \times L)$, where U_{air} and P_{rz} are the external flow velocity and the pressure in recirculation

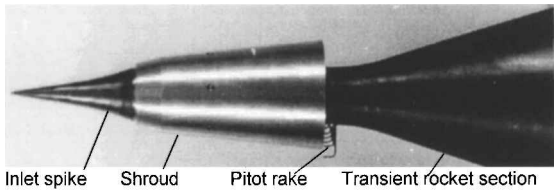

Fig. 6 Photos of small-scale engine channel with transient nose rocket section.

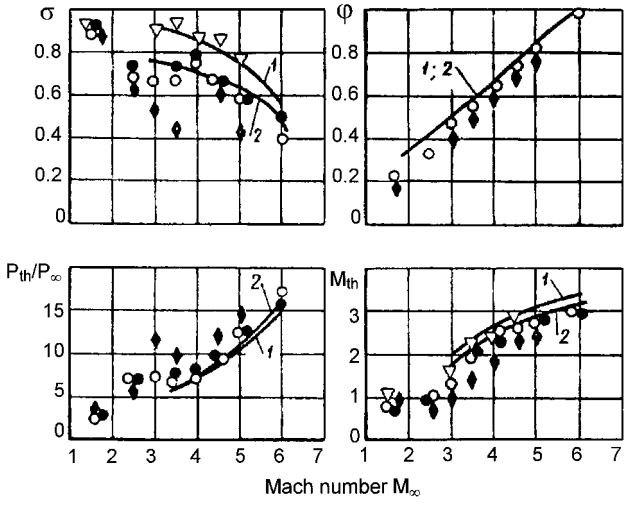

Fig. 7 Axisymmetrical inlet performance ($\alpha_{at} = 0$ deg): 1, 2-calculation data without and with taking into account boundary layer[6]; Experimental data: ∇, core Pitot rake; ○, through cross section Pitot rake; ●, mass-averaged flow; ♦, mass-averaged flow with throttling at φ_{max}.

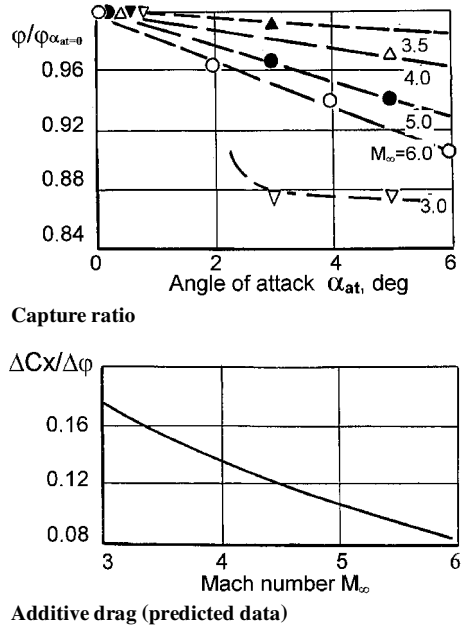

Fig. 8 Effect of attack angle on experimental inlet performance.

zone, was proposed taking into consideration airflow parameters, the cavity length L, and fuel/air equivalence ratio β_{rz} in cavity (see Fig. 9).[5] It is possible to extract three main regions of combustion: the first one is the residual flame region, when the combustion takes place only within the cavity; the second one is the flame spreading region outside the cavity, which supports by the combustion in the cavity; and the third one is selfignition region. This criterion was obtained under the following flow and geometric parameters:

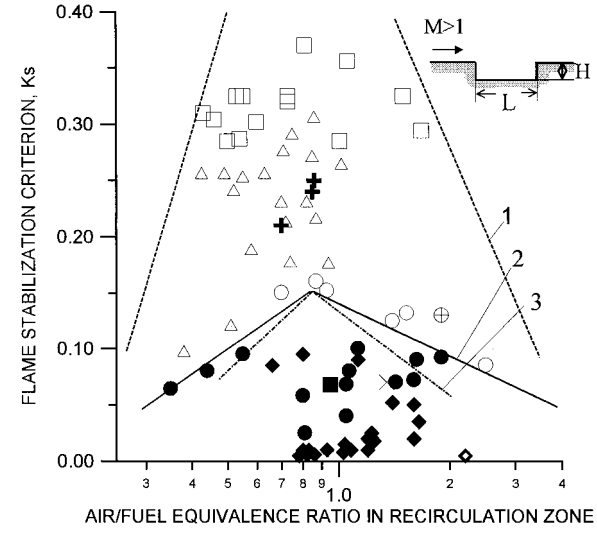

Fig. 9 Generalization of experimental data on ignition and combustion stabilization process: open—○, □, △, +, ⊕—and solid—■, ♦, ●—symbols correspond to regimes of residual flame and flame spreading and self-ignition; boundaries of 1, residual flame; 2, spreading flame; 3, self-ignition.

$M = 2$–3, $T_{t,air} = 800$–1400 K, $P_{rz} = 7$–100 kPa, $L = 20$–70 mm, $s/d = 3$–8 (relative distance between fuel injectors of d diameter), and $T_{rz}/T_{air} = 0.9$–3.6.

Analysis of experimental data on the burning of hydrogen jets, injected from wall or struts, allowed the development of semiempirical relationships for combustion efficiency[6,7] as a function of generalized parameters. For both relationships the main parameters were the number of fuel nozzles, air/fuel equivalence ratio, relative combustor length and its expansion ratio. In accordance with Ref. 6, the mixing and combustion efficiency depends on the uniformity of fuel/air distribution within the combustor and on the pressure rise in the combustor. It was found also that combustor expansion gives rise to combustion efficiency decrease and at certain conditions even to flame extinction as a result of the kinetic factors.[6]

C. DMSCRAM Nozzle

Research into the nozzle was not the aim of the first-stage flight test because of the peculiarities of the engine installation on the rocket and the absence of thrust measurement. However, based on parametric numerical researches of nozzle flowfield (two-dimensional and axisymmetrical), the nozzle profile and nozzle expansion ratio were chosen in such a way that the ratio of nozzle-exit area to inlet entrance area was equal to two. The characterisitcs of SCRAM noncontrollable nozzle operation in the off-design regime (flow Mach numbers and specific heat ratio at nozzle entrance are variable) and effect of flow nonuniformity and chemical nonequilibrium processes[8] on nozzle performance were obtained. Results on the nozzle/combustor operation were obtained by carrying out axisymmetrical DMSCRAM tests.

D. Engine Cooling System and Hydrogen Consumption Control System

A parametric design study of the DMSCRAM convective-cooling system was conducted under ground- and flight-test conditions. Based on experimental data, variations in heat-transfer processes and the maximum thermal-loading location along the engine duct were determined. A generalized mathematical model was developed based on solutions of gas-dynamic and heat-transfer equations for the processes in the engine duct and jacket of cooling system. Numerical research of the DMSCRAM cooling system under permissible wall temperature $T_{w,max} = 1100$ K and stationary flight conditions of $M = 5$ (shown in Fig. 10) indicated that much more cooler cooling flow is needed than the fuel flow required during the supersonic mode combustion at $\beta = 0.3$–0.6. The normalized cooling

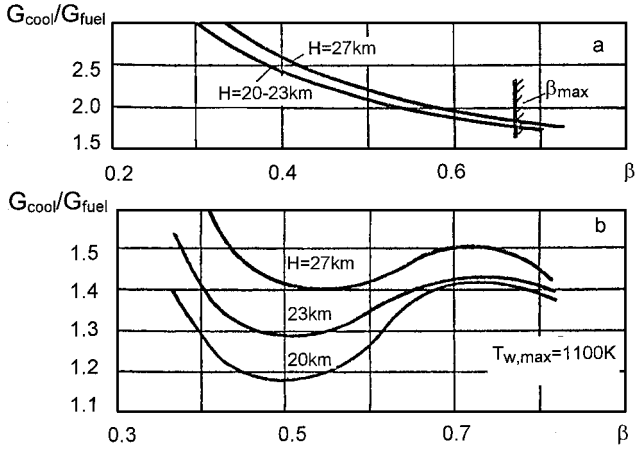

Fig. 10 Axisymmetrical DMSCRAM cooling system performance at $M_\infty = 5$ for supersonic a and subsonic combustion modes b.

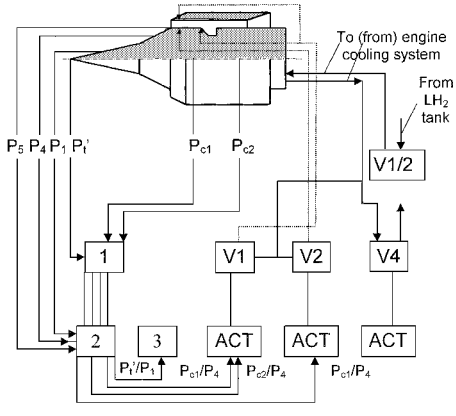

Fig. 11 Control system architecture of DMSCRAM.

flow rate, $\bar{G}_{\text{cool}} = G_{\text{cool}}/G_{\text{fuel}}$ ranges from 1.75 to 3.0. During the subsonic-mode combustion ($\beta = 0.3$–1.1), less cooler consumption is needed, with $\bar{G}_{\text{cool}} = 1.2$–$1.5$. Satisfactory agreement between predicted and experimental data was confirmed using the methods developed for analysis of nonstationary flight data.[9] During the flight, the excess fuel used for cooling was removed through the holes circumferentially placed on the rocket transition section, and it was controlled by the fuel regulator in accordance with the control system operation. In the case of ground tests of engines with cooling system under the limit on hydrogen flow rate, a test method based on the use of liquid nitrogen or air as a cooler was suggested.

A control system for hydrogen consumption and its distribution in the injectors rows is necessary for the DMSCRAM flight tests. Design and experimental investigations of the hydrogen-fueled engine and mathematical modeling of the engine control system allowed the generation of control laws, programs, and parameters.[10] For its realization without direct hydrogen consumption measurement, a closed-loop nonstatic control system with fluidic components was used. Two ratios of the combustor pressures (p_{c1} and p_{c2}) to the engine inlet pressure (p_4) have been used as control parameters: $p_{c1}/p_4 = F_{c1}(M)$ and $p_{c2}/p_4 = F_{c2}(M)$. The control system functions were flight Mach-number measurement, control programs generation, change of gaseous hydrogen consumption and its distribution in sub- and supersonic combustion modes, prevention of disgorgement of the shock from the engine inlet ("shock-out" mode), and provision of additional combustion chamber wall cooling. Figure 11 shows schematically the structure of the engine control unit. The control system consists of a unit for measuring the freestream and combustor pressures, p'_t, p_{c1}, and p_{c2} (i.e., pos. 1), intended for forming the hydrogen consumption control commands and for changing the combustor operating mode (sub- or supersonic combustion); a unit for the fluidic components (i.e., pos. 2) for comparison of the reduced pressures with the p_1 and p_4 values and for logic operations execution according to the engine control program; a Mach-meter unit (i.e., pos. 3) that determines the flight Mach number as a function of p'_t/p_1 and provides program values of $F_{c1}(M)$ and $F_{c2}(M)$ through the use of profiled cams; a piston-type actuators assembly (i.e., pos. ACT) to drive flow throttling valves V1 and V2 for modifying the consumptions to three injector rows and valves V1/2 and V4, which supply the hydrogen flow to the combustor cooling jacket. The V4 valve is operated on the cooling jacket walls according to the overheat signal.

The experimental investigations of the control system unit has been carried out for ground tests with a simulated control loop (the aggregates are full scale, and the engine model is on the analog computer) at $M = 3.5$–5.5 and $H = 16$–26 km. It was established that the system operation stability is ensured by special selection of the motion-valve angular velocities and of the fluidic component gains. The test results were good for the static control parameters, for the engine shock-out modes simulated with the $p_5 > p_4$ signal, for the transient regimes from the subsonic to supersonic combustion mode and vice versa, and for compensation of the fuel-consumption intensive perturbations.

E. Liquid Hydrogen Storage and Supply Systems

Design, construction, and experimental investigations of LH_2 feeding, storage, and supply systems were conducted within the framework of the ground equipment and launch system preparation for flight test by CIAM together with the Design Bureaus "Fakel," Scientific Industrial Company "Kryogenmash," and others. Model, mock-up, and real LH_2 tanks protected by screen-vacuum insulation, control devices, valves, and other equipment for He-pressurized fuel tank and fuel supply control systems were fabricated and tested. Based on the test data analysis, the LH_2 losses for precooling of HFL system were evaluated as 10–15% of tank volume during daytime. Also the necessary preparations and tests of external feeding system and control devices were carried out.

V. Ground Tests of Model and Flight-Type DMSCRAM

The main objectives for the first USSR ground test of a full-scale model DMSCRAM were 1) to determine the operation characteristics at the sub- and supersonic modes of combustion, 2) to obtain experience on engine and experimental data analysis methods, and 3) to make recommendations for designing the flight-type engine. Tests of DMSCRAMs were carried out at the CIAM test benches with gaseous hydrogen ($T_{\text{fuel}} = 300$ K) under freejet conditions (BMG test bench) at $\alpha_{\text{at}} = 0$ deg and $M = 5$ (sub- and supersonic combustion modes) and $M = 6.2$–6.4 (supersonic combustion modes) and direct-connect conditions (Ts-101 test bench) with simulation of flight parameters, corresponding to $M = 3.5$–4.0 (subsonic combustion modes). At $M = 5$, the freestream flow stagnation parameters were $T_t = 900$–1200 K and $P_t = 1.8$–2.5 MPa; at $M = 6.2$ these parameters are $T_t = 1300$–1600 K and $P_t = 4.4$–5.8 MPa; and at $M = 3.5$–4.0 entering flow Mach number was ≈ 2.0 and $T_t = 750$–1000 K, $P_t = 0.15$–0.24 MPa. Heating of air was provided by vitiated (kerosene fueled heater at BMG), resistance-, and arc-type heaters (Ts-101). For initiation of combustion, the sparkplugs were used, and as a rule their operation continued during the whole run.

Ground tests of the flight-model DMSCRAM were carried in freejet environments (BMG) corresponding to $M = 5$ and altitude $H = 25$ km conditions. Schematics of the two-dimensional DMSCRAM installation at BMG and Ts-101 test benches are presented in Fig. 12. Installation of the axisymmetrical DMSCRAM was analogous. The flight engine was tested in two variants: the first was with the use of 10 separate flow metering nozzles for checking of the airflow rate and the second without metering nozzles for checking of combustion operation. The data acquisition system included pressure gauges, thermocouples, gas sampling probes, fuel, air and water mass flow meters and shadow device. Thrust forces were measured during the tests at Ts-101. Determination of the averaged flow parameters and engine thrust performance was conducted with the use of one-dimensional processing methods of experimental data. Reliability of such approaches was confirmed by methodical

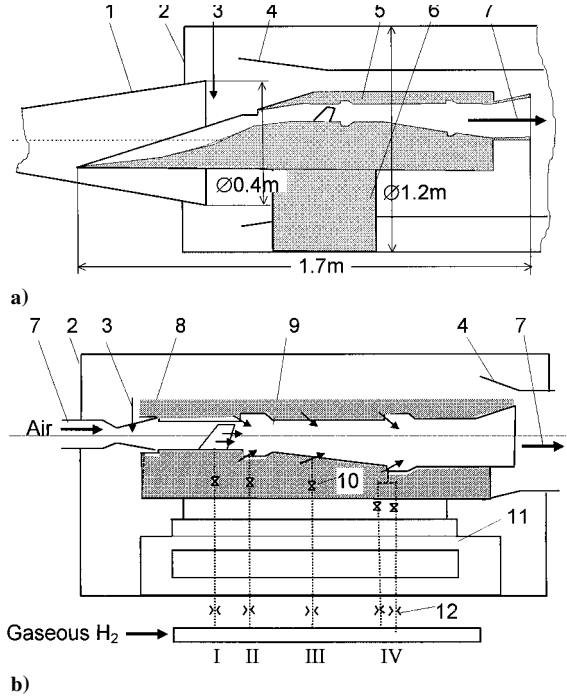

Fig. 12 Schemes of two-dimensional DMSCRAM ground test: a) free-jet test bench (BMG) and b) direct-connect pipe line (Ts-101). 1, wind-tunnel nozzle; 2, vacuum chamber; 3, combined pitot tube and T_t probe; 4, exhaust diffusor; 5, two-dimensional DMSCRAM; 6, support strut; 7, to exhauster; 8, direct-connect unit; 9, DMSCRAM combustor; 10, valve; 11, thrust-balance device; 12, fuel-metering nozzle, I, II, III & IV—rows of fuel injectors.

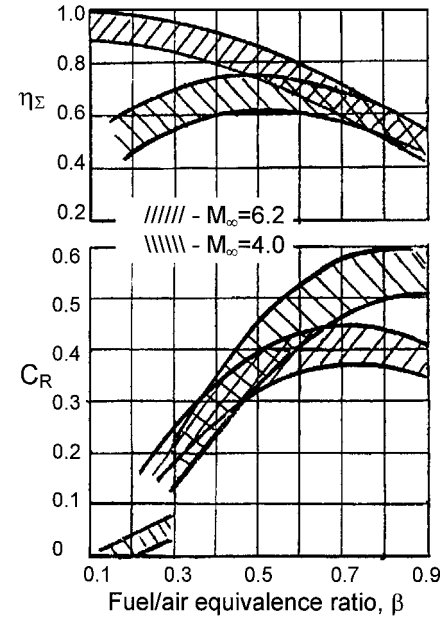

Fig. 13 Two-dimensional scramjet performance.

investigations and good correlation of the gas-dynamic and thrust methods.

Main results of the model DMSCRAM researches were given in Refs. 3, 11, and 12.

A. Two-Dimensional DMSCRAM

Researches of two-dimensional DMSCRAM mock-up at $M = 6.3$ confirmed the possibility of full-scale DMSCRAM tests at the BMG test bench under design and off-design ("shock-out" mode) conditions by means of a special throttling device installed at the engine exit section. It was found that rather rapid equalization of the pressure nonuniformity along the duct occurred even at the average supersonic velocity at the combustor exit, which additionally argues in favor to processing with the use of the one-dimensional methodology.

In tests corresponding to supersonic combustion mode, when fuel was injected in the first combustor section, two critical values of the fuel/air equivalence ratios β were obtained. The first one (β_{cr}) defines the fuel consumption, when the increase of it results in changes of the flowfield in the combustor, which leads to subsonic combustion zone in the first combustor section and thermal choking at the exit of this section. The second one (β_{max}) corresponds to the maximum fuel consumption beyond which a normal shock appears in the upstream of the cowl. In the second and third combustor sections the average flow is supersonic. Startup of engine with ignition and stabilization of combustion was provided at all β values and different fuel distribution between the injector rows. Combustion efficiency η_{comb} in the combustor exit section is decreased when the β value is increased (see Fig. 13) corresponding to diffusion combustion. The main part of fuel burns in the first section, with the remaining in the second and third sections (approximately with equal efficiencies), that gives an evidence of decreased mixing and combustion in the extended sections in comparison with processes in the section $F = \text{const}$. Measurements showed that the maximum heat transfer was observed in the first section cavity flameholders and behind them ($q_{w,max} = 2.5$–3.3 MW/m^2). The maximum value of q_w, however, was observed also at the bottom wall between the fuel pylons, which is an evidence of fuel combustion in the separation zones ahead of the fuel injectors. The total value of heat fluxes $\bar{Q}_w$ to the combustor walls relative to the heat resulting from the fuel combustion varied from 25–30% at $\beta = 0.1$ down to 12–14% at $\beta = 0.7$–0.8.

Stable subsonic combustion mode regimes were realized over a wide range of $\beta = 0.16$–1.0 and under different techniques of engine startup. It was shown that, at small M and high altitude H, startup is achieved by a short-duration increase of airflow parameters P and T. Maximum fuel consumptions, which did not result in off-design flow of inlet and nonstable inlet/combustor operation, were determined. Peculiarities of gas-dynamic flow structure in the flowpath and effect of fuel distribution between the fuel injector rows on this structure were found. The combustion efficiency η_{comb} depended on the total fuel consumption and was almost independent of on the fuel distribution between the injector rows (Fig. 13). This indicated that the increase of η_{comb} caused by preliminary hydrogen mixing in the upstream of the combustion zone was negligible. The main reasons for low η_{comb} were the short length of the third section, non-uniform distribution of fuel injected through the fourth fuel row along the cross section, and small depth of fuel penetration into the main flow at the third section. $\bar{Q}_w$ value on these regimes is equal to 5–11% from heat resulting from combustion.

Thrust performance of DMSCRAM was obtained with the use of freestream conditions and flow parameters in the engine flowpath accounting for the off-design cowl flow. It was assumed that engine nozzle had $\bar{F}_{eng} = F_{noz}/F_{inl} = 2$, and the losses of exit flow impulse were 2%. Also the return of the heat transferred into the duct walls was taken into account. Values of thrust coefficients are shown in Fig. 13.

B. Axisymmetrical DMSCRAM

The investigation of axisymmetrical DMSCRAM was carried for two stages. Main results were obtained during the first stage when fuel was supplied only through I and II injector rows placed on the central body of the first combustor section to provide supersonic mode combustion. In case of the subsonic mode, the fuel was supplied through III and IV injector rows placed at the end of second and at the beginning of third combustor sections. However, in these runs a large degree of hydrogen non uniformity was observed along the duct cross sections, which was confirmed by the gas sampling analysis data, the wall-temperature distribution, and the heat-flux measurements. To eliminate this imperfection, the V injector row was fabricated and placed at the end of the first combustor section on the cowl for the second stage tests. Results of researches with some

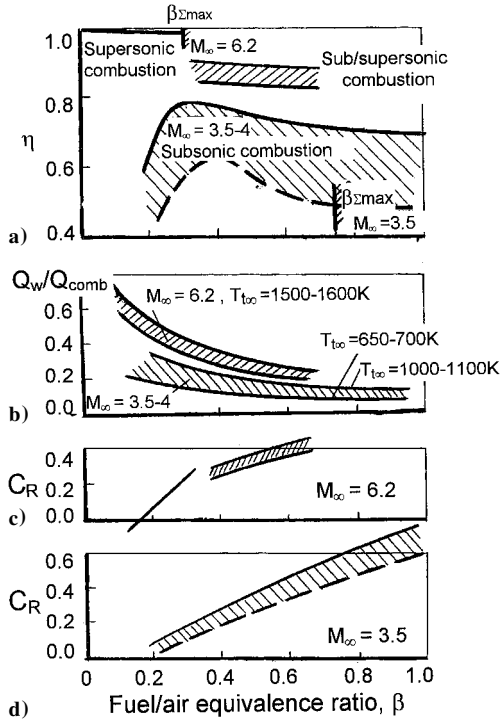

Fig. 14 Generalized results of the axisymmetrical DMSCRAM experimental investigation.

hydrogen injection through the V row (I + V, III + V etc.) confirmed a more uniform distribution of hydrogen along the duct and gave an appreciable increase of η_{comb} values.

The increase of the relative combustor length and number of the fuel injectors resulted in an increase of the η_{comb} values in comparison with the two-dimensional DMSCRAM ones (Fig. 14a). However, the total hydraulic pressure losses increased considerably because of the large wetted surface of the annular combustor and because of the thick struts placed in the duct, especially in the supersonic combustion regimes. So at $M = 6.2$ runs, the flow was supersonic only for $\beta_{max} < 0.3$. When $\beta > 0.3$, combustion was realized in the extended part of the chamber at subsonic velocities. Some hydrogen was injected through the III or V rows at $\beta > 0.3$ because of the decrease of β_{cr}. At $M = 3.5$ and subsonic combustion regimes the value of $\beta_{max} \approx 0.75$ characterizes the limiting fuel consumptions through the III injector row when the flow at the combustor entrance is not changed. The increase in the wetted surface caused an increase of $\bar{Q}_w$ almost twice that for the two-dimensional engine (Fig. 14b), although these results were obtained without accounting for heat transfer in the nozzle duct.

Thrust performance was counted with the use of experimental data in the same way as for two-dimensional DMSCRAM (Figs. 14c and 14d). It was proposed that at $M = 6.2$, the inlet capture ratio φ is 1, while $\varphi = 0.54$ at $M = 3.5$ and a possible decrease of φ at $\beta > \beta_{max}$ was not accounted for. According to preliminary researches, the nozzle impulse losses were accepted as 3.5%.

C. Flight Version of DMSCRAM

The ground tests of the flight version of DMSCRAM at $M \approx 5$ were an important step for the preflight tests. The ignition of hydrogen in the combustor, determination of inlet parameters in engine assembling, operation of the cooling system and methodology of testing the cooled DMSCRAM were checked during these tests. To determine the mass flow rate through the engine, a special metering nozzle device was developed and fastened at the engine nozzle exit. The system for model cryogenic liquid coolant (liquid nitrogen, air, or its mixture) was developed, fabricated, and tested.

The tests proved the possibility of DMSCRAM starting at $\beta = 0.7$–0.8 with hydrogen ignition by electrical sparkplugs and stable combustion by cavity flame stabilizers (Fig. 15a). The

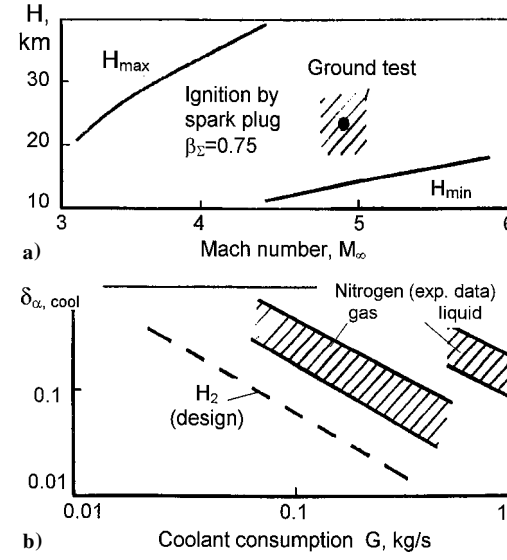

Fig. 15 Ground-test results of flight type DMSCRAM: a) start engine test (ignition of hydrogen fuel at sub- /supersonic regimes) and b) cooling system test.

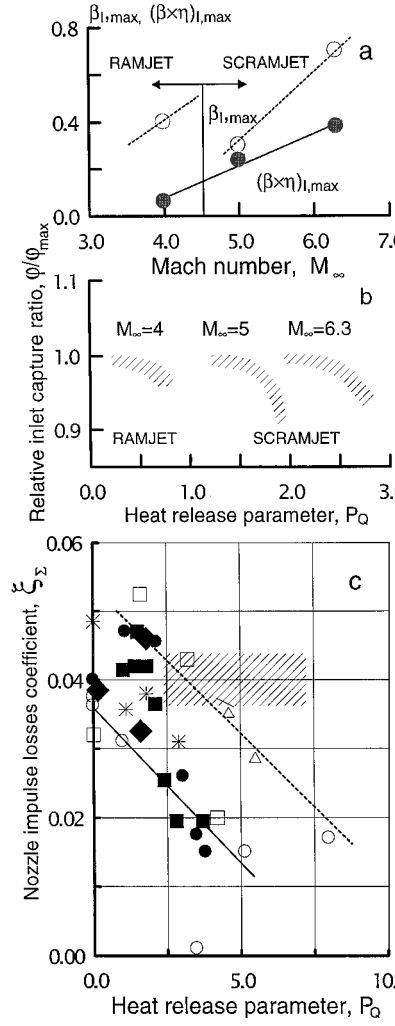

Fig. 16 Joint inlet/combustor and nozzle/combustor operations: a) maximum heat-release parameters (two-dimensional DMSCRAM)— β_I and $(\beta \times \eta)_I$ vs Mach number; b) two-dimensional engine air capture ratio vs first combustor section heat-release parameter $P_{QI} = (\beta \times \eta)_I \times 10^4/T_t$; c) nozzle impulse loss coefficient, ξ_Σ vs $P_{Q\Sigma}$ (axisymmetrical engine); ●, ○—$g_{III} = G_{fIII}/G_{f\Sigma} = 1$; ■, □—$g_{III} = 0.4, g_{IV} = 0.6$, △, ∗—$g_{II} = 0.6, g_{III} = 0.4$; ♦—$g_I = 0.1, g_{II} = 0.9$; ////—(calculation under test conditions).

experimental value for the inlet capture ratio was found to be close to the theoretical value and to the model test data. The dynamic and hydraulic characteristics of the cooling system were determined, and its durability was confirmed for the summary operation time in the test cell of about 200 s, with ≈60–70 s of combustion runs. It was established by the tests that even for the primary parts of cooling shell, a sufficiently uniform coolant distribution was achieved along the perimeter of the annular channel. This statement confirms the data on nonuniformity degree for heat-transfer coefficient α in the cooling channel, characterized by $\delta_{\alpha,\text{cool}} = (\alpha_{\max} - \alpha_{\min})/\alpha_{\text{average}}$ at the end of the combustor, as shown in Fig. 15b. Here, $\alpha_{\max}$, $\alpha_{\min}$, and α_{average} are maximal, minimal, and average heat-transfer coefficient values in different measuring points of cooling channel.

The final checkout of DMSCRAM durability was done in the first flight test in November 1991.[13]

D. Peculiarities of Joint Elements Operation in Engine Assembling

During the model engine tests, problems of the combined inlet, combustor, and nozzle operation were revealed in engine assemblies, which were insufficiently investigated at autonomous tests. The data on the combined inlet/combustor operation are shown in Figs. 16a and 16b for the rectangular DMSCRAM.[3] The data show the variation of the capture ratio $\varphi/\varphi_{\max}$ as a function of the heat-addition parameter P_Q in the first section of the combustor, defined as $P_{\text{QI}} \sim \beta_{\text{I}} \times \eta_{\text{I,comb}}/T_{t,\text{air}}$ and the ultimate fuel mass flow rate $\beta_{\text{I,max}}$ as a function of the freestream Mach number.

More data were obtained on hydrogen ignition and flame stabilization by cavity stabilizers for the combined combustors of DMSCRAM. Some new data were obtained on the thermal condition of cavity stabilizers. All data obtained on the heat-transfer coefficient were generalized using a relationship in the form of $Nu = f(Re)$, which correlates with the experimental data without combustion.

The tests on the operation of the axisymmetric engine nozzle together with the combustor revealed the influence of the combustor on the nozzle, defined as the Mach-number variation by the flowfield variation at the combustor exit. Figure 16c shows the impulse-loss coefficient as a function of the heat-release parameter in the combustor $P_{Q,\text{comb}}$. It is likely that this relationship becomes different for another engine.

VI. Summary

As part of the development and preparation of the DMSCRAM flight tests, detailed investigations and tests were conducted of both the individual elements and the engine systems, as well as their joint operations in the engine environment. The data obtained provided a basis for the recommendations for the flight version of the DMSCRAM and for performing flight tests for the first time.

Acknowledgments

The authors are sincerely grateful to the participants of this work from CIAM, Design Bureaus "Soyuz," "Fakel," "EGA," and SIC "Cryogenmash" for their assistance and collaboration.

References

[1] Iiiff, K. W., and Shafer, M. F., "A Comparison of Hypersonic Flight and Prediction Results," AIAA Paper 93-0311, Jan. 1993.

[2] Sosounov, V. A., "Study of Propulsion for High Velocity Flight," *Proceedings of the Xth International Symposium on Air Breathing Engines*, Sept. 1991.

[3] Vinogradov, V. A., Grachev, V. A., Petrov, M. D., and Shikhman, Yu. M., "Experimental Investigation of 2-D Dual Mode Scramjet with Hydrogen at Mach 4-6," AIAA Paper 90-5269, Oct. 1990.

[4] Vinogradov, V. A., Duganov, V. V., and Stepanov, V. A., "Application of Numerical Methods for Designing of Super- and Hypersonic Inlets," *Journal of TsAGI Scientific Notes*, Vol. 13, No. 2, 1982, pp. 62–68 (in Russian).

[5] Strokin, V. N., and Grachev, V. A., "Possible Schemes of Flameholding in Hydrogen Fueled Scramjet Combustors," *Proceedings of the First International Aerospace Congress*, Vol. 1, Academy, Moscow, 1997, pp. 630–633.

[6] Strokin, V. N., and Grachev, V. A., "The Peculiarities of Hydrogen Combustion in Model Scramjet Combustors," *Proceedings of the XIII International Symposium on Air Breathing Engines*, Vol. 1, AIAA, Reston, VA, 1997, pp. 374–384.

[7] Annushkin, Yu. M., "Main Dependencies of Turbulent Hydrogen Jets Combustion in Air Duct," *Journal of Physics of Combustion and Explosion*, Vol. 17, No. 4, 1981, pp. 59–71 (in Russian).

[8] Khailov, V. M., "Chemical Relaxation in Jet Engine Nozzles," *Mashinostroenie*, Moscow, 1975, p. 228 (in Russian).

[9] Antonov, A. N., Shikhman, Yu. M., Shlaykotin, V. E., and Tchivanov, S. V., "Mathematical Simulation of Scramjet Operation with Convective Cooling System Under Non-Stationary Heating of Construction," *Proceedings of the XX Readings on Cosmonautics*, Russian Academy of Sciences, Moscow, 1996, pp. 58, 59 (in Russian).

[10] Aparin, E. L., Belukov, A. A., Stepanov, G. P., and Shikhman, Yu. M., "Parameters and Control System of Experimental Dual-Mode Scramjet," *Proceedings of the First International Conference on Airspace "Man-Earth-Space," Session of Propulsion for Airspace System*, Vol. 4, Russian Engineering Academy, Mashinostroenie, Moscow, 1995, pp. 435–449 (in Russian).

[11] Albegov, R. V., Kurziner, R. I., Petrov, M. D., and Shikhman, Yu. M., "Operation Process Peculiarities in Combined Combustor Under Heat Addition into Sub- and Supersonic Flow," *Proceedings of the Readings Devoted to F.A. Tsander's Works, Session of Aviation Engine Theory*, Russian Academy of Sciences, Kuibishev, 1985, pp. 95–106 (in Russian).

[12] Vinogradov, V. A., Albegov, R. V., and Petrov, M. D., "Experimental Investigation of Hydrogen Burning and Heat Transfer in Annular Duct at Supersonic Velocity," *Physics of Combustion and Explosion*, No. 6, 1991, pp. 24–29 (in Russian); also International Council of the Aeronautical Sciences, Paper 92-3.4R2, Sept. 1992.

[13] Kandevo, S. W., "Russian Want U.S. to Join Scramjet Test," *Aviation Week and Space Technology*, Vol. 136, No. 13, March 1992, pp. 18–20.